Hough Transform and Active Contour for Enhanced Iris Segmentation

Alaa Hilal[1,2], Bassam Daya[2] and Pierre Beauseroy[1]

[1] UMR STMR – LM2S – ICD, Université de Technologie de Troyes, Troyes, 10004, France

[2] IUT, Université Libanaise, Saida, Liban

Abstract

Iris segmentation is considered as the most difficult and fundamental step in an iris recognition system. While iris boundaries are largely approximated by two circles or ellipses, other methods define more accurately the iris resulting in better recognition results. In this paper we propose an iris segmentation method using Hough transform and active contour to detect a circular approximation of the outer iris boundary and to accurately segment the inner boundary in its real shape motivated by the fact that richer iris textures are closer to the pupil than to the sclera. Normalization, encoding and matching are implemented according to Daugman's method. The method, tested on CASIA-V3 iris images database is compared to Daugman's iris recognition system. Recognition performance is measured in terms of decidability, accuracy at the equal error rate and ROC curves. Improved recognition performance is obtained using our segmentation model proposing its use for better iris recognition system.

Keywords: *Iris segmentation, Biometric, Hough transform, Active contour.*

1. Introduction

Biometric systems that recognize human features are often used for personal identification. Their main applications are in surveillance, security, identification and verification of individuals for controlling access to secured areas or materials. These systems extract and identify unique biometric features such as finger prints, palm prints, hand shape, retinal vasculature, handwritten signature, shape of the ear and voice. Since most of the existing methods have limited capabilities in recognizing relatively complex features in realistic practical situations, research and development are into more robust identification systems such as iris based recognition system. In fact Iris recognition system is considered among the most recent and reliable biometric human recognition systems [1]. The iris, considered as an internal organ yet externally visible, has unique, complex and stable features that do not change over time since 8 months after the birth [1].

Many processes lead the iris to be recognized; with no direct contact and a little human cooperation, an image of the eye is taken. The iris is first segmented, isolating it from the rest of the image. The segmented iris is then normalized to take into account scale and camera-eye distance variation. Normalized iris is encoded after it to define iris signature that is ready to be matched. Since the first complete implementation of the system by Daugman [2] and till our days, many researchers approve that iris segmentation is the most difficult and one of the most important step in the process [1], [2], [24], [28], [29].

While normalization, coding and iris matching are of common interest, they are all related to the segmentation process. Iris segmentation should be robust to closed eyelids, eye lashes, specular reflections and, in the non-ideal cases, the deviated gaze images. It should be able to isolate the iris and extract it accurately.

In the following paragraphs, we present a literature review on iris segmentation then we introduce the proposed method and its implementation. Next the results are presented and compared to Daugman's results to finish with conclusions.

2. Segmentation review

Iris is a disk bounded by the pupil from inside and by the sclera and the eyelids from the outside. In most commercial systems and advanced researches, the iris is modeled by two non-concentric circles [1], [2]. The algorithm scans the eye image to detect these two circles; then extracts the eyelids by some model approximation and remove eyelashes and specular reflections using intensity threshold. We present in what follows a classification of different proposed methods in iris segmentation.

Daugman was the first to present a complete iris recognition system [1]. To segment the iris he defined the so-called Daugman Integro-differential operator as follow:

$$\max_{(r,x,y)} \left| \frac{\partial}{\partial r} G_\sigma(r) * \int_{r,x,y} \frac{I(x,y)}{2\pi r} ds \right| \quad (1)$$

where $I(x,y)$ represents the image intensity at location (x,y), $G_\sigma(r)$ is a radial σ scale Gaussian smoothing filter, s is the contour of the circle (x, y, r) and * denotes for convolution. The operator searches for the circle where there is maximum change in pixel values, by varying the radius r and center (x, y) position of the circular contour s. Two maximum values are obtained corresponding to the two circles defining the iris. Daugman doesn't use any thresholds on the gradient image, what makes all image information usable. But from the other side, the operator becomes more sensitive to noisy values which may lead to wrong iris detection. As for eyelids, Daugman uses parabolic operator. The operator searches and detects parabolic curve that models the eyelids. Finally eyelashes and specular reflections are isolated by intensity threshold.

Wildes introduced the circular Hough transform to detect the iris [3]. The algorithm calculates the image gradient creating an edge map to be transformed into Hough space. Votes are then calculated to define two circles given a range of possible radius. Outer iris boundary is detected before inner boundary. The results are sensible to the defined gradient image and to the predefined range of possible circle radius. Wildes also used parabolic Hough transform to detect the eyelids and intensity threshold to isolate the eyelashes.

In his work [4], Masek implemented Wildes' segmentation method. He used Canny edge detection to detect iris edge points. Vertical edges are used to detect the outer iris boundary at first after it horizontal edges detect inner iris boundary. To separate eyelids from the iris, a horizontal line obtained after a linear Hough transform application on the image isolates each eyelid from the iris. Eyelashes and specular reflections are segmented by intensity threshold.

In [5]-[10], iris segmentation is based on Hough transform. In [5], Mahlouji et al. utilized circular Hough transform to segment the iris. Using Circular Hough transform applied to an edge map created by a Canny filter, the inner iris boundary is first detected then the outer boundary is detected after it. After it, linear Hough tranfrom is used to exclude eyelids. Results reported in a recognition accuracy of 97.50%.

In [8], iris segmentation is based on Masek's implementation of Wildes' segmentation. Compared to Wildes method, the iris detection order is reversed; the pupil is first detected then the outer iris boundary. A second modification is in eliminating very high intensity edge points as they are possibly originated from specular reflections. Upper and lower eyelids are also detected using Wildes' method, but they are divided into two equal parts. And instead of modeling each eyelid by a horizontal line, the eyelid is now modeled by two connected lines.

Some researchers [11]-[15] used ellipse fitting to segment the iris especially in the case of off angle images. In [11], a non-cooperative iris segmentation algorithm is introduced. The method is based on numerically stable direct least squares fitting of ellipses model and modified Chan-Vese model. The iris boundaries are fitted with an ellipse in a first stage, next they are accurately segmented using a modified Chan-Vese model. Better segmentation efficiency with lower processing time is reported using CASIA V3 images.

Ryan et al. [15] used Starburst algorithm, introduced in [16], to detect limbic and pupil boundary. Eyelids are detected using snake algorithm. Better results in iris segmentation are reported but the number of parameters to adjust and search increased (major and minor axis length, center coordinates and rotation angle).

In [17] and [18] iris is localized by use of Morphologic operators like intensity threshold, opening and closing. More specifically in [17] intensity information is used to find a square region that completely surrounds the pupil. The square region is then binarized to extract an edge map from it. An iterative morphological operator's algorithm is then applied to detect the iris inner boundary. Outer boundary is divided into right and left sides in which they are detected by arched Hough transform and finally merged together. Obtained results claim to show an improvement in the precision of the iris localization. But it must be taken into account that the database used to test the methodology (CASIA - Version 1) is considered as an easy non challenging database.

Other methods based on circular iris boundaries approximation also have been implemented such as least square method proposed by Zhu et al. [19] and gray-scale distribution feature method proposed by Yuan et al. [20], [21]. Other methods as well are based on ellipse fitting such as Zuo and Natalia [22].

Active contours are also used to detect irises [2], [23]-[29]. Many approaches are used to apply parametric or nonparametric models to segment the iris boundaries, [23]-[25]. In [26], a semantic iris contour map combining spatial information on iris location (obtained by a circular Hough transform) and gradient map as edge indicator is

used for level set active contour segmentation. The semantic iris contour map is claimed to reduce the local extremes in iris region misleading the evolution of the iris contour. Tests were performed on ICE (2005) database and CASIA V3 database, reporting efficient and effective results.

In [2], gradient vector flow is used to implement the active contour segmentation. Pupil is first segmented with an initial circle containing the pupil. Then an ellipse containing the iris is used as initial contour to segment the outer iris boundary. Chen et al. used probabilistic active contour [27], Daugman used Fourier coefficients based active contour [23] and Shah and Ross [28] made use of geodesic active contours for iris segmentation. Vatsa et al. [29] used a modified energy function to detect the exact iris boundaries by evolving the initial contour in narrow bands.

3. Proposed Methodology

An analysis of the iris segmentation literature shows that iris segmentation is divided into circle/ellipse fitting or real contour detection. According Huang et al. [30] investigations, the actual iris boundaries are not always circular; while the outer iris boundary is so close to a circle, it is not the case for the inner boundary. In addition iris richer textures are closer to the pupil than to the sclera [2]. These two facts explain the importance to accurately define and segment the inner iris boundary; the pupil must be correctly isolated from the iris without identifying some pupil boundaries as belonging to iris region. As for the external iris boundary, a circular approximation fits enough the real shape especially that the iris region close to the sclera is poor with important textures.

In our method we propose to detect the pupil-iris boundary in its real shape and the iris-sclera boundary in a circular approximation. Circular Hough transform detects at first the outer iris boundary, defines a region of interest ROI that contains the pupil and after it applied again to the ROI, it gives a circular approximation of the pupil's boundary. Then active contour without edges model is applied using the circular inner iris boundary approximation as an initial contour to accurately segment the inner iris boundary in its real shape. We describe in what follow the circular Hough transform, the active contour model and their implementation.

2.1 Circular Hough transform

Hough Transform is an algorithm that permits to detect objects in an image within a certain geometrical form as a line, circle, ellipse… We are interested here in circular Hough transform that detects circular shapes. To do so a binary edge map is first generated, by use of a gradient filter. Then, votes in a circular Hough space are analyzed to estimate the three parameters of a circle: center (x_0,y_0) and radius (r) [3]. The parameters of the circle to be detected are modeled as the following circle equation:

$$(x-x_0)^2+(y-y_0)^2=r^2 \quad (2)$$

The location (x_0, y_0, r) with the maximum value of Hough space is chosen as the parameter vector for the strongest circular boundary.

2.2 Active contour without edges

Active contour is a dynamic curve that evolves iteratively toward object contour in an image. An energy function describes the contour by its physical properties (connectivity, curvature, balloon …) and by the properties of the image (gradient, intensity…). The algorithm finds a combination between image pixels to minimize the energy function in order detect the contour. Many models exist for active contour; each defining a different energy function. In our method we used active contour without edges model that detects the contour of an image without calculating its gradient and eventually its edges [31].

To describe this model, figure 1 [32] shows an image of a single object having different color intensity from its background. C_0 is the object's real contour, c_1 and c_2 are respectively the average intensities inside and outside C_0 and $U(x,y)$ is the intensity value in pixel (x,y) The active contour energy is defined as:

$$F(c_1,c_2,C)=F_1(C)+F_2(C)=\sum_{Interior(C)}|U(x,y)-c_1|^2+\sum_{Exterior(C)}|U(x,y)-c_2|^2 \quad (3)$$

According to F we can have four different cases of detected contour as shown in figure 2 [28].

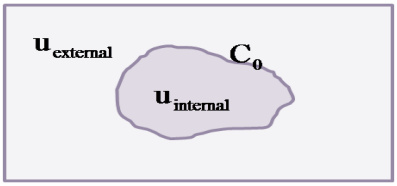

Fig. 1 Image representing a single object of intensity $U_{internal}$, separated by the contour C_0 from its back ground of intensity $U_{external}$.

By taking the four different cases of figure 2, we combine all possible outcomes of the green contour with the real one [26]:

$$F_1(C) > 0 \,\&\, F_2(C) \approx 0 \quad (4)$$

$$F_1(C) \approx 0 \,\&\, F_2(C) > 0 \quad (5)$$

$$F_1(C) > 0 \,\&\, F_2(C) > 0 \quad (6)$$

$$F_1(C) \approx 0 \,\&\, F_2(C) \approx 0 \quad (7)$$

It is clear that minimizing *F* leads to the detection of the contour. And the problem of contour detection simplifies to be solution of minimizing F in terms of c_1, c_2 and C. Starting with an initial contour *C*, the contour evolves into the direction of minimizing *F* and detecting the real contour according to the differential equation given by Chan et al. [31]:

$$\frac{\partial C(x,y)}{\partial t} = div\left(\frac{\nabla C(x,y)}{|\nabla C(x,y)|}\right) - (U(x,y) - c_1)^2 + (U(x,y) - c_2)^2 \quad (8)$$

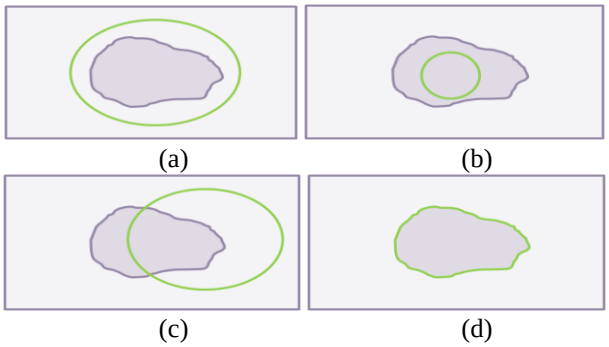

Fig. 2 Four different cases of detected contour.

2.3 Implementation

Starting with an eye image, outer iris boundary is firstly segmented by circular estimation using circular Hough transform. The result obtained helps to define the pupil ROI. Then circular Hough transform is applied once again to approximate the pupil by a circle to be used as an initial contour for active contour segmentation. The image has a big size, rich iris texture complexity and contains different heterogonous regions inside of it, which will mislead the active contour. Thus by defining the pupil ROI and an initial contour which is close to the real boundary the space search for the inner iris boundary will be decreased, eventually saving processing time and increasing speed of convergence of the active contour. For active contour implementation, we adopted the discretization of Eq. (8) used by Chan et al. in their work [31].

A condition for active contour convergence must be set. This means imposing a convergence criterion to stop the active contour when global minimum of energy function F is obtained. To do so, we measure the variation within iterations of the pupil's region surface. Convergence is obtained when the pupil's region becomes almost stable and varies within a small interval.

Specular reflections inside the pupil may mislead the active contour. To overcome this problem, pixels inside of the pupil are subject to a low pass filter that neglects high intensity values coming from specular reflections. This is sufficient since high contrast exist between the dark pupil and the very light specular reflections.

For eyelashes and eyelids noise removal, we used Wildes method. Search for a linear Hough transform detects upper and lower eyelids. From each of the detected lines, a horizontal line refines and excludes the eyelids. As for eyelashes, they are excluded by intensity threshold.

In order to compare and evaluate the efficiency of the segmentation, we compared our proposed model with the reference model of Daugman. We kept the normalization, encoding and matching unchanged and we used the same models used with Daugman.

Once segmented iris is normalized according to 'Rubber Sheet' model proposed by Daugman [1]. Daugman approximates the iris with a circular ring. He normalizes the iris patterns by projecting the iris into a dimensionless rectangular shape. Intensity pixels $I_c(x,y)$ in the Cartesian space of the segmented iris are mapped to the Pseudo-Polar space $I_p(r,\theta)$ by the following equations:

$$I_p\{r,\theta\} = I_c\{x(r,\theta), y(r,\theta)\} \quad (9)$$

$$x(r,\theta) = (1-r)x_p(\theta) + rx_s(\theta) \quad (10)$$

$$y(r,\theta) = (1-r)y_p(\theta) + ry_s(\theta) \quad (11)$$

where $(x_p(\theta), y_p(\theta))$ and $(x_s(\theta), y_s(\theta))$ are the coordinates of the internal and external iris boundaries respectively at angle θ. r varies from 0 to 1 corresponding respectively to the internal and external iris circular boundaries and θ varies from 0 to 2π.

Encoding of the iris textures is ensured by 2D Gabor filters, same proposed and used by Daugman. It provides an excellent attributes which are very suitable to extract iris features. A 2D Gabor filter over an image domain is given by:

$$G(r,\theta) = e^{-i\omega(\theta-\theta_0)} e^{-(r-r_0)^2/\alpha^2} e^{-i(\theta-\theta_0)^2/\beta^2} \quad (12)$$

where (α,β) specify the effective width and length and ω is the filter's angular frequency having (r_0,θ_0) the center frequency. The convolution of the normalized iris image with 2D Gabor filter results in complex valued coefficients. Using Daugman's phase quantization method, the phase information of these coefficients is quantized into four levels, one for each possible quadrant in the complex plane [1].

Finally Hamming distance as defined by Daugman [1] is used for the matching stage, it is used to determine whether two iris codes belong to the same person or not. Let A and B be two iris codes to be matched. The Hamming distance (HD) is calculated as follows:

$$HD = \min_{\varphi}\left\{\frac{1}{M \times N}\sum_{i=0}^{M}\sum_{j=0}^{N}\left(A(i+\varphi, j) - B(i, j)\right)\right\}$$

$$\text{for } -10 \le \varphi \le 10 \qquad (13)$$

where M and N are respectively the angular and radial size of the iris code. φ is a rotational parameter that compensate for iris rotation and *Min* is the minimum outcome of the equation in parentheses. The lower value outcome is the HD. The Hamming distance is considered as a similarity score between two iris images. A HD value that is lower than a threshold indicates that the two images match [1].

3. Results

To test our method, CASIA V3-Interval images were used [33]. The iris data base contains 2639 iris images captured from 249 subjects. Most of the images were captured in two sessions, with at least one month interval. The images are in 8 bit grayscale JPEG files, collected under near infrared and having a resolution of 320 * 280 pixels. They are considered as a good quality iris images with clear iris texture details. In figure 3 two iris images shows that the pupil's shape is far from being neither a perfect circle nor a perfect ellipse. We used these images to demonstrate and explain the difference in the two segmentation approaches.

In figure 4, the two segmentation methods are shown on each iris image at the same time. The white circle is the circular approximation segmentation while the green contour is result of our proposed segmentation method.

The obtained results show that the external iris boundary is well described by a circle. The circular approximation fits the external iris boundary. Eyelashes and eyelids that overlay the iris would be isolated subsequently.

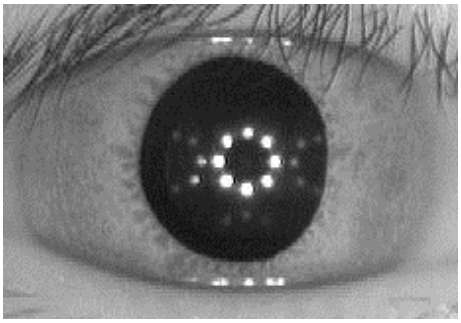

(a)

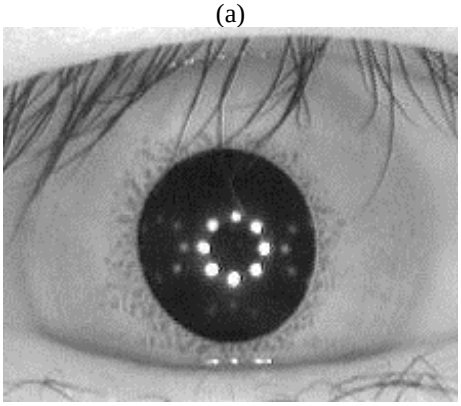

(b)

Fig. 3 Two iris images showing a non circular pupil.

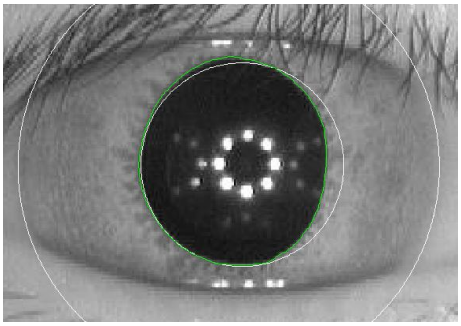

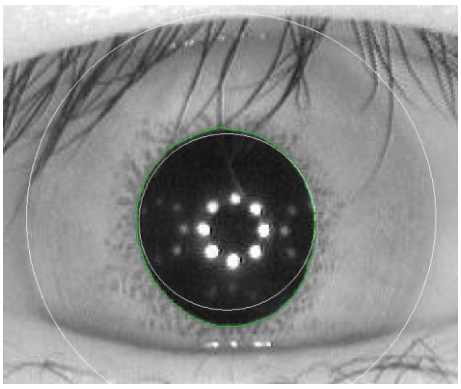

Fig. 4 Iris images segmented with circular approximation in white contour and with active contour in green contour.

As for the inner iris boundary, the pupil is not well described and segmented with a circle. Within the white detected circle, a part of iris region is considered as belonging to the pupil and at the same time a part of the pupil, exterior to the white circle, is considered as iris region. Wrong identification such this can influence the recognition performance. On the other hand, the green contour, result of our segmentation, accurately detects the pupil in its real shape.

After the iris has been segmented, eyelashes and eyelids still need to be isolated. Linear Hough transform is used to detect upper and lower eyelids, it permits to define two horizontal lines that exclude the eyelids. As for eyelashes, they are segmented by intensity threshold. The images in the datasets used, have irises with intensity values generally higher than 100, while eyelashes have intensity values lower than 100. An intensity threshold of 100 is then set to isolate the eyelashes.

To define the convergence criterion of active contour, we measured the variation of pupil region with iterations. Figure 5 shows this variation in typical pupil segmentation in two cases of the images in figure 3.

In figure 5(a), the first image of figure 3 is segmented; the initial active contour evolves to detect the real pupil boundary. The active contour's region decreases with iterations to reach an almost fix level. The pupil's region is less than that defined with its circular approximation. While segmenting the second image of figure 3, the active contour's region increases with iterations as shows figure 5(b). In this case the pupil's region is bigger than its circular approximation. In both images of figure 5, starting from about the 45^{th} iteration the active contour region varies within a range of 20 pixels. The active contour is almost stable indicating convergence to pupil segmentation.

The algorithm is tested on the entire iris data base. Error in segmentation occurred when eyelashes are covering or masking a part of the pupil.

Figure 6 shows a case where the model fails to segment the iris. In 6(a), the pupil is heavily covered by eyelashes misleading the active contour to accurately identify and detect the pupil. Figure 6(b) shows the detected boundaries where the covering eyelashes are identified as region of the pupil. The segmented iris is shown in figure 6(c).

Eyelashes and eyelids are eliminated according to the methodology already described. Even if the segmentation considered some eyelashes as part of the pupil, it didn't introduce noisy data to the iris affecting matching decision.

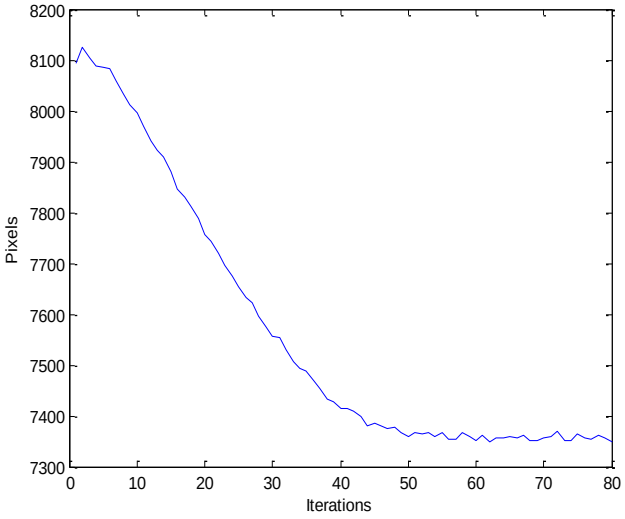

(a)

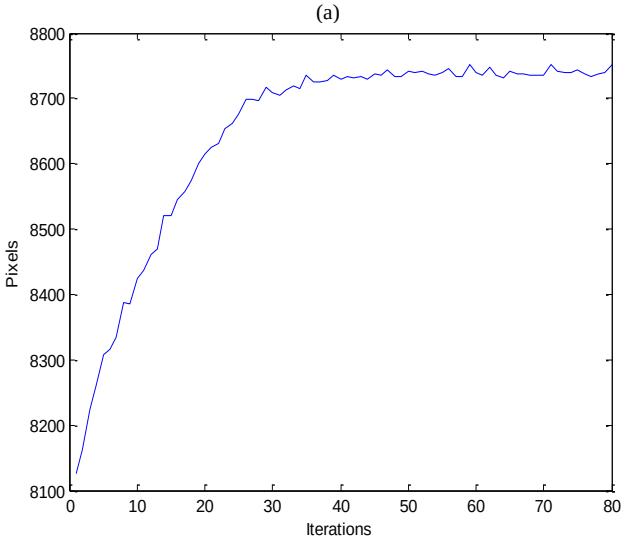

(b)

Fig. 5 Variation of active contour region along iterations during the segmentation of the two images of figure 3. In 5(a), the pupil from figure 3(a) is smaller than its circular approximation, active contour's region decreases with iterations to detect it accurately. While in 5(b) it is the opposite case; the pupil from figure 3(b) is bigger than its circular approximation. Active contour's region increases with iterations to detect the pupil.

After segmentation, iris is normalized according to Daugman's rubber sheet model. Iris is transferred into the polar space with a stable dimension of 32 (radial resolution) * 240 (angular resolution) pixels. 2D Gabor filter is then applied to encode irises features.

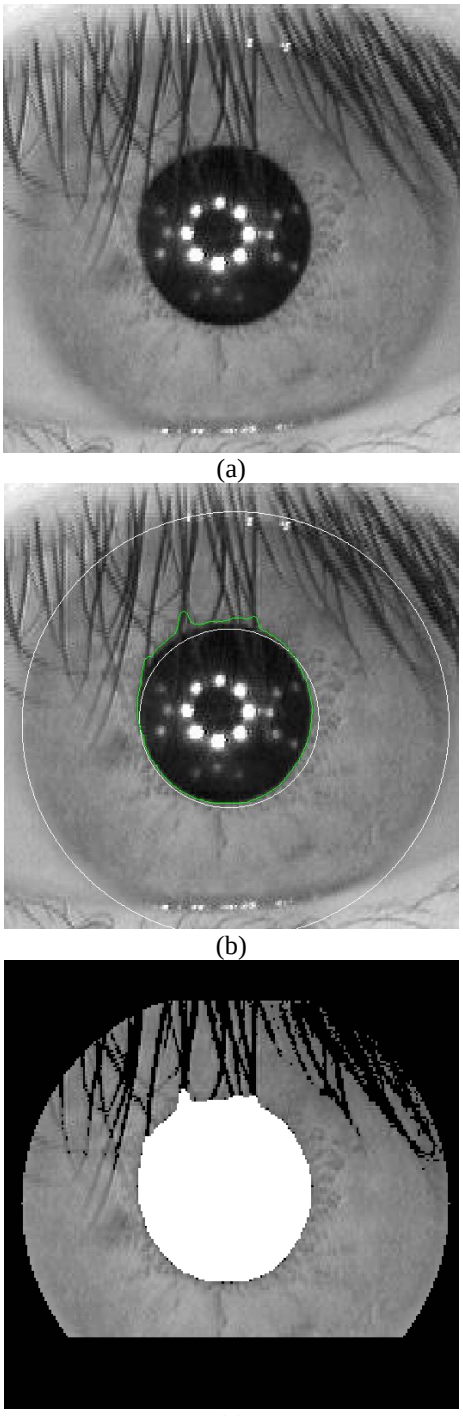

(a) (b) (c)

Fig. 6 Segmentation of highly covered iris. (a) Iris covered with eyelashes; (b) Detection of the iris; (c) Segmented iris.

To evaluate the proposed segmentation effect and its contribution in recognition results, recognition performance is measured. Three recognition performance parameters are calculated namely, decidability, accuracy at the equal error rate and ROC curves.

Decidability is a performance parameter proposed and used for the first time by Daugman [1]. It measures the separation between the inter and the intra-class distributions of the Hamming distances. Intra-class HD distribution is the outcome of comparing irises that belong to same person whether inter-class is the HD values of comparing irises of different persons from the dataset. The decidability is given by the following equation:

$$Decidability = \frac{|\mu_S - \mu_D|}{\sqrt{(\sigma_S^2 + \sigma_D^2)/2}} \quad (14)$$

Where μ_S and μ_D are respectively the intra and inter-class distribution's mean, while σ_S and σ_D are respectively the standard deviations of the intra and inter-class distributions. Daugman's system resulted in a decidability of 6.41 while our real shape pupil segmentation based iris recognition system resulted in a higher decidability value which is 7.26. Our system separates better between the two distributions.

Second performance parameter is the accuracy at equal error rate (EER). It is accuracy achieved when the false accept rate (FAR) and false reject rate (FRR) are equal. FAR measures the probability of a person being wrongly identified as another individual while FRR the probability of an enrolled person not being identified by the system [4].

Let $s^D_{i,j}$ be an inter-class score HD calculated between samples i and j of two different persons and $s^S_{i,j}$ be the intra-class score HD. FAR and FRR can be calculated for a threshold *T* according to the following equations [2]:

$$FAR(T) = \frac{\left|\left\{s^D_{i,j} \le T\right\}\right|}{\left|\left\{s^D_{i,j}\right\}\right|} \quad (15)$$

$$FRR(T) = \frac{\left|\left\{s^S_{i,j} \ge T\right\}\right|}{\left|\left\{s^S_{i,j}\right\}\right|} \quad (16)$$

where |…| is the cardinal of a set.

Figure 7 shows the FAR, FRR curves and EER for the two recognition systems. Daugman's system resulted in an equal error rate of 0.0027 that corresponds to an accuracy of 99.73% for a 0.4066 threshold, while our system resulted in same equal error rate value and thus same accuracy but with a lower threshold of 0.3758.

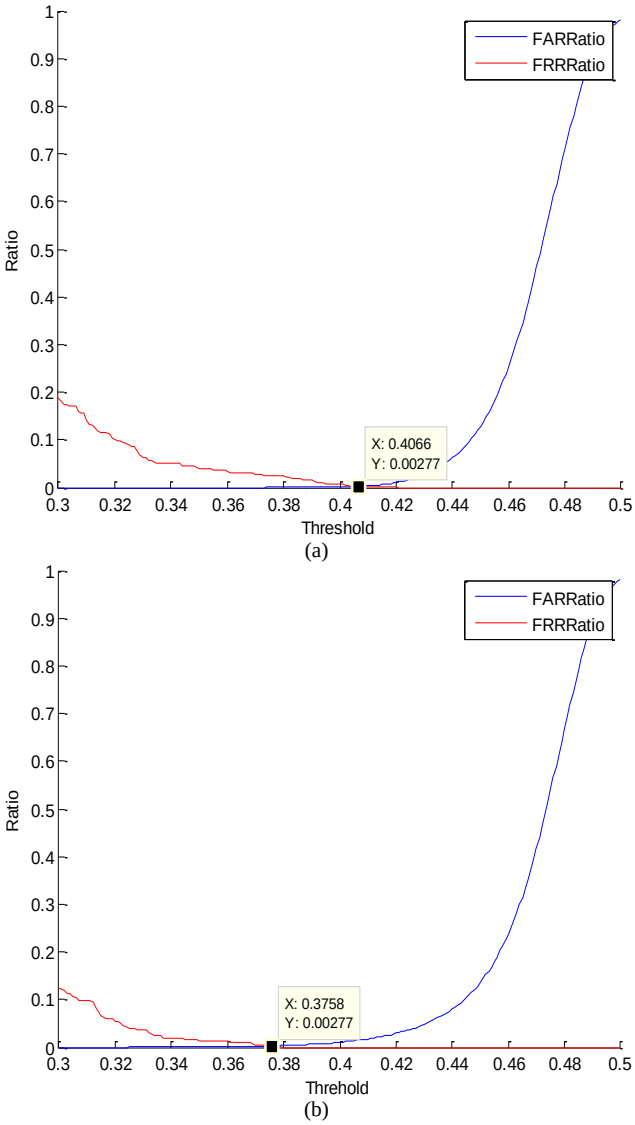

Fig. 7 FAR, FRR curves and EER value for Daugman's system in (a) and for our proposed system in (b).

Receiver operating characteristics (ROC) curves is the third performance parameter used to evaluate our system. The ROC curves give the best analyses of accuracy because they present the achieved accuracy over a range of operating points. ROC curves are obtained by presenting the FAR variation in terms of FRR. More an ROC curve is asymptotic to the abscissa and to the ordinate axes, better are the system's performances [2]. Figure 8 show the ROC curves obtained with the two systems. Our system's ROC curve is more asymptotic to the abscissa and ordinate axes than Daugman's ROC curve showing that our segmentation affected the recognition performance and improved accuracy at most operating points, especially at low operating points where significant accuracy improvements are shown.

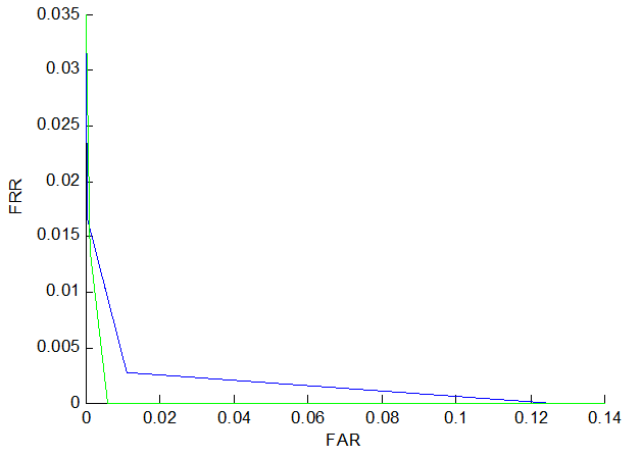

Fig. 8 ROC curves for Daugman's system in blue curve and green curve for our system.

The three obtained performance parameters for both systems are summarized in table 1 below.

Table 1: Performance parameters of Daugman's and our recognition iris system

Performance parameter	***Our system***	***Daugman's system***
Decidability	7.26	6.41
Accuracy at EER	99.73%	99.73%
ROC curves	More asymptotic curve	Less asymptotic curve

4. Conclusions

In this paper we proposed an iris segmentation methodology for the purpose of iris recognition. The proposed method segments accurately the inner iris boundary in its real shape. The effect of the segmentation on iris recognition results is measured using three performance parameters: decidability, accuracy at the equal error rate and ROC curves. Compared to Daugman's system, where iris inner boundary is approximated to a circle, our proposed system resulted in same accuracy at EER but better decidability and ROC curves. Results obtained encourage the use of the proposed segmentation methodology for an improved performance iris recognition system.

Acknowledgments

Portions of the research in this paper use the CASIA-IrisV3 collected by the Chinese Academy of Sciences' Institute of Automation (CASIA).

References

[1] J. Daugman, "High confidence visual recognition of persons by a test of statistical independence", IEEE Transactions on Pattern Analysis and Machine Intelligence, Vol. 15, No. 11, 1993, pp. 1148-1161.

[2] E. Krichen, "Reconnaissance des personnes par l'iris en mode dégradé", PhD thesis, Evry-Val Essonne University, 2007.

[3] R. P. Wildes, " Iris recognition: An emerging biometric technology ", Proceedings of the IEEE, Vol. 85, No. 9, 1997, pp. 1348-1363.

[4] L. Masek, "Recognition of human iris patterns for biometric identification", B.S. thesis, The School of Computer Science and Software Engineering, The University ofWestern Australia, CrawleyWA, Perth, Australia, 2003.

[5] S. V. Dhavale, "Robust Iris Recognition Based on Statistical Properties of Walsh Hadamard Transform Domain",IJCSI International Journal of Computer Science Issues, Vol. 9, No 2, 2012.

[6] M. Mahlouji and A. Noruzi, "Human Iris Segmentation for Iris Recognition in Unconstrained Environments", IJCSI International Journal of Computer Science Issues, Vol. 9, No 3, 2012.

[7] S. Nithyanandam, K. S. Gayathri, P. L. K. Priyadarsini, "A New IRIS Normalization Process For Recognition System With Cryptographic Techniques", IJCSI International Journal of Computer Science Issues, Vol. 8, No 4, 2011.

[8] X. Liu, K. W. Bowyer, and P. J. Flynn, "Experiments with an improved iris segmentation algorithm", in Proc. of IEEE 4th Workshop on Autom. Identification and Advanced Technologie, 2005, pp. 118–123.

[9] Q. Tian, Q. Pan, Y. Cheng, and Q. Gao, "Fast algorithm and application of Hough transform in iris segmentation", in 3rd Int. Conf. Mach. Learn. Cybern., 2004, vol. 7, pp. 3977–3980.

[10] C. L. Fancourt, L. Bogoni, K. J. Hanna, Y. Guo, R. P. Wildes, N. Takahashi, and U. Jain, "Iris recognition at a distance", in Int. Conf. AVBPA, 2005, pp. 1–13.

[11] M. Elsayed, M. Mansour, H. Saad, "Non cooperative Iris Segmentation", IJCSI International Journal of Computer Science Issues, Vol. 9, No 1, 2012.

[12] E. Sung, X. Chen, J. Zhu, and J. Yang, "Towards non-cooperative iris recognition systems", in Proc. of 7th ICARCV, 2002, vol. 2, pp. 990–995.

[13] K. Miyazawa, K. Ito, T. Aoki, K. Kobayashi and H. Nakajima, "An effective approach for iris recognition using phase-based image matching", IEEE Transactions on Pattern Analysis and Machine Intelligence, Vol. 30, No. 10, 2008, pp. 1741-1756.

[14] J. Zuo, N.K. Ratha and J.H. Connell. "A new approach for iris segmentation", in IEEE Computer Society Conf. on Computer Vision and Pattern Recognition Workshops (CVPRW'08) 2008.

[15] W. Ryan, D. Woodard, A. Duchowski, and S. Birchfield, "Adapting starburst for elliptical iris segmentation", in Conf. BTAS, 2008, pp. 1–7.

[16] T. A. Camus and R. P. Wildes, "Reliable and fast eye finding in closeup images", IEEE 16th Int. Conf. on Pattern Recognition, 2004, pp. 389-394.

[17] H. Ghodrati, M. J. Dehghani, M. S. Helfroush, "Localization of Noncircular Iris Boundaries Using Morphology and Arched Hough Transform", 2nd International Conference Image Processing Theory Tools and Applications (IPTA), 2010; pp. 458-463.

[18] J. De Mira, Jr. and J. Mayer, "Image feature extraction for application of biometric identification of iris - A morphological approach", in 16th Proc. Symp. Comput. Graph. Image Process, 2003, pp. 391–398.

[19] Y. Zhu, T. Tan, Y. Wang, "Biometrics personal identification based on iris pattern", in 15th Int. Conf. on patern recognition, 2000, Vol. 2, pp.801-804.

[20] W. Q. Yuan, L. Xu, Z.H. Lin, "Iris localization algorithm based on gray distribution features of eye images", Journal of Optoelectronics-Laser, Vol. 17, No, 2, 2006, pp.226-230.

[21] W. Q. Yuan, J. F. Ma, W. B. Di, "A new method of iris location based on the active contour", Journal Computer Engineering and Application, Vol. 40, No. 34, 2003, pp. 104-107.

[22] J. Zuo, A. Natalia, "On a methodology for robust segmentation of nonideal iris images", IEEE Trans. Syst. Man Cybern. B, Vol. 40, No. 3, 2010, pp. 703–718.

[23] J. Daugman, "New methods in iris recognition", IEEE Trans. Syst., Man, Cybern. B, Cybern., Vol. 37, No. 5, 2007, pp. 1167–1175.

[24] J. Daugman, "Probing the uniqueness and randomness of iriscodes: Results from 200 billion iris pair comparisons", Proc. IEEE, Vol. 94, No. 11, 2006, pp. 1927–1935.

[25] X liu, "Optimizations in Iris Recognition", PhD thesis, University of Notre Dame, 2006.

[26] X. Zhang, Z. Sun, T. Tan, "Texture removal for adaptive level set based iris segmentation", Proceedings of IEEE 17th International Conference on Image Processing, 2010.

[27] R. Chen, X. Lin, T. Ding, J. Ma, "Accurate iris segmentation Applied to Portable Image Capture Device", International Workshop on Imaging Systems and Techniques, 2009, pp. 80-84.

[28] S. Shah, A. Ross, "Iris Segmentation Using Geodesic Active Contours" IEEE Transactions on Information Forensics and Security (TIFS), Vol. 4, No. 4, 2009, pp. 824-836.

[29] M. Vatsa, R. Singh, A. Noore, "Improving Iris Recognition Performance Using Segmentation, Quality Enhancement, Match Score Fusion, and Indexing", IEEE Transactions on Systems, Man, and Cybernetics, Part B: Cybernetics, Vol. 38, 2008, pp.1021 -1035.

[30] J. Huang, X. You, Y. Y. Tang, L. Du, "A novel iris segmentation using radial-suppression edge detection", Signal Processing, Vol. 89, No. 12, 2009, pp. 2630-2643.

[31] T. F. Chan, L. A. Vese, "Active contours without edges", IEEE Transaction on image processing, Vol.10, No.2, 2001, pp. 266-277.

[32] A. Hilal, A. Chaddad, J. Charara, "Segmentation des cellules cancéreuse du colon: une nouvelle approche", International Conference on Advances in Biomedical Engineering ICABME, 2011.

[33] CASIA-IrisV3, http://www.cbsr.ia.ac.cn/IrisDatabase.htm"

Alaa Hilal received the BS degree in general physics in 2008 and the MS degree in medical imaging in 2010 both from the Lebanese University, Lebanon. He is currently working toward the PhD degree at the Lebanese University, Lebanon and the University of Technology of Troyes, France. He is actively involved in the development of robust iris recognition system. He has 3 publications in international conferences and journals. His current areas of interest include image processing, pattern recognition and biometrics.

Bassam Daya received the BE degree in electrical and computer engineering in 1992 from the Lebanese University, Lebanon, the MS degree in automatic control and applied computer in 1993 from the Ecole Centrale of Nantes, France and the PhD degree in automatic control and applied computer in 1996 from the University of Angers, France. He was an assisting professor from 1994 till 1998 in the University of Angers, France and worked as a research engineer from 1996 till 1998 in UNIVALOIRE Society, Angers, France. From 1998 till 2002 he was an assistant professor at the Lebanese University, IUT of Saida, Lebanon and after it an associated professor from 2002 till 2007 in the same university and he became since 2007 a full professor in the Lebanese university. He was awarded one of the top ten graduates of the 1991-1992 academic year presented by the cultural center Hariri in 1992 at the American University of Lebanon, Lebanon. He obtained the first prize in the annual competition LIRA of the Lebanese industrial research achievements of 2004 between all Lebanese universities on programming and telecommunications section. He obtained as well the third prize in the same section of the same competition LIRA for both years 2004 and 2005. He was the chief of many projects organized by CEDAR and Ministry of culture in Lebanon in 2006 and in 2009. He is the co-other of the best paper award on the 30th international conference on information systems, architecture and technology, Poland, 2009. He has more than 44 published papers. His current research interests are in neural network architecture for robotics systems, object detection and identification (face, vehicle, and elderly fall detection), iris recognition, learning Rules in the Purkinje cell system of the cerebellar cortex and its application to a bipedal robot.

Pierre Beauseroy received his engineering degree in computer science and his master degree in complex system control from University of Technology of Compiegne in 1988. He received his PHD degree in complex system control from the same university in 1992. Since 1993 he is continuing his research at the University of Technology of Troyes. He is a full professor since 2010 and leads the system modeling and dependability team (LM2S) since 2011. His major research interests are pattern recognition and machine learning.